

KfK 2734
Dezember 1978

A Proton Microbeam Deflection System to Scan Target Surfaces

D. Heck
Institut für Angewandte Kernphysik

Kernforschungszentrum Karlsruhe

KERNFORSCHUNGSZENTRUM KARLSRUHE

Institut für Angewandte Kernphysik

KfK 2734

A Proton Microbeam Deflection System
to Scan Target Surfaces

D. Heck

Kernforschungszentrum Karlsruhe GmbH, Karlsruhe

Als Manuskript vervielfältigt
Für diesen Bericht behalten wir uns alle Rechte vor

Kernforschungszentrum Karlsruhe GmbH
ISSN 0303-4003

ABSTRACT

A system to deflect the proton beam within the Karlsruhe microbeam setup is described. The deflection is achieved within a transverse electrical field generated between parallel electrodes. Their tension is controlled by a pattern generator, thus enabling areal and line scans with a variable number of scan points at variable scan speed. The application is demonstrated at two different examples.

Ein Protonen-Mikrostrahl-Ablenksystem für die Abtastung von Probenoberflächen.

ZUSAMMENFASSUNG

Ein System zur Ablenkung des Protonenstrahls innerhalb der Karlsruher Mikrobeam-Anordnung wird beschrieben. Die Ablenkung geschieht in einem transversalen elektrischen Feld zwischen parallelen Elektroden. Deren Spannung wird von einem Bildmuster-generator kontrolliert, der flächen- und linienhafte Abtastung mit einer variablen Anzahl von Analysenpunkten bei variabler Abtastgeschwindigkeit erlaubt. Die Anwendung wird an zwei verschiedenen Beispielen gezeigt.

<u>CONTENTS</u>	<u>PAGE</u>
1. Introduction	1
2. Deflection Units	1
2a. Horizontal Deflector	1
2b. Vertical Deflector	2
3. Scanning Pattern Generator	3
4. Application Examples	4
Acknowledgement	5
Literature	5
Figures	6

1. INTRODUCTION

To analyze the spatial distribution of the elemental composition in a target surface with the aid of a proton microbeam, the beam spot position must be moved relative to the target surface. This may be done (a) by displacing the target (e.g. by means of a stepping motor drive), or (b) by sweeping the beam across the surface. The latter method enables a much higher variation speed, thus local target heating by the beam can be minimized. In comparison with a scanning electron microscope, the beam particles have much higher energies (up to some MeV) and greater masses ($m_p/m_e \sim 2000$) and suffer only negligible deflections by iron-free magnetic coils. Iron-filled coils must be excluded, as magnetic hysteresis destroys an unambiguous relation between coil current and deflection. Therefore, beam deflection by a transverse electric field generated by appropriately dimensioned high voltage electrodes is preferred.

2. DEFLECTION UNITS

2a. Horizontal Deflector (Y-direction).

A particle of the energy E_0 and charge e_0 passing through an electrical condenser (d = distance between the plates, l = length of the plates, U = tension between the plates) with the electrical field perpendicular to the flight path of the particle suffers a deflection by the angle α . For small angles ($\alpha \sim \text{tg}\alpha$) the deflection from the original direction is given by

$$\alpha \approx \frac{e_0}{E_0} \cdot \frac{l}{d \cdot 2} U \quad (1)$$

This relation has to be applied to the conditions of the microbeam^{1,2}): The maximum particle energy E_0 is ~ 4 MeV, the maximal length of deflecting plates is given by the distance between the exit of the second quadrupole and the entrance flange of the target chamber and amounts to ~ 6.5 cm. A beam spot shift of ± 250 μm on the target at a distance of 12.5 cm from the center of the plates corresponds to a deflection angle of ± 2 mrad. With equation (1) this results in a field gradient of

$$\frac{U}{d} \approx \pm 2.5 \text{ kV cm}^{-1}$$

At a plate gap of 0.8 cm the plates must be brought to opposite tension of ± 1 kV to get this gradient. The use of two voltage sources of opposite sign for the two plates offers the advantage that the midplane between the plates rests at ground potential, thus the fringe field effects at the entrance and exit are minimized. To get an homogeneous deflecting field, the front side of the plates is chosen as large as possible to 2.8 cm (which is 3.5 times the gap width). It is limited by the diameter of the beam tube.

2b. Vertical Deflector (X-direction).

Because of the limited space between the exit of the second quadrupole and the target, a different solution is chosen for the deflection in vertical direction. When the entrance slit of the microbeam system is shifted from position O to O' (see Figure 1) the beam spot on the target surface moves from I to I' with the relation

$$II' = M * OO' \quad (2)$$

where M is the magnification factor of the lens system. One must keep in mind, however, that with increasing distance from the optical axis the influence of image aberrations increases the spot size diameter.

For the case of the Karlsruhe microbeam system²⁾, the slit shifts are calculated to ± 0.58 mm. Vertical slit shifts cause an additional coma aberration of ≈ 0.5 μm , while other additional aberrations are negligible.

In practice the slit is not shifted, but two pairs of deflecting electrodes are arranged between the entrance slits and the first quadrupole lens at the positions P_1 and P_2 , which bring the beam along the dashed-dotted path of Figure 1. By a suitable choice of the length of the electrodes it can be achieved that the central ray crosses the axis of the system at the position of the principal plane H, when the appropriate electrodes of the two deflectors are held at the same tension. With the distances $l_1 = 19.8$ cm and $l_2 = 114$ cm the resulting electrode lengths are 10.4 and 20 cm. With 1 cm gap width at 6.5 cm front edge length, an homogeneous electric field is generated in the middle of the deflection condensers. For 4 MeV particle energy, deflection tensions of ± 110 V are sufficient for a beam spot shift of ± 250 μm .

In such a system the aperture angle remains unchanged when the aperture diaphragm is placed in the principal plane. This is possible, since in the case of a quadrupole doublet the principal planes are well outside the lenses.

In a final remark it should be pointed out that this principle of double deflection cannot be applied in the horizontal direction, as the much larger distance $O - O'$ of 7.35 mm causes tremendous additional aberrations (distortions $\sim 75 \mu\text{m}$, astigmatism $\sim 40 \mu\text{m}$, coma $\sim 8 \mu\text{m}$). In test measurements with the horizontal and vertical deflection system as described above, no significant enlargement of the spot size of $3 \mu\text{m}$ diameter³⁾ could be observed, even at beam spot displacements of $400 \mu\text{m}$ from the system axis.

3. SCANNING PATTERN GENERATOR

To avoid local heating of the target, it is recommended to use a high scan speed for the sweeping across the region of interest on the target surface. As shown in the previous section, deflection voltages up to 1 kV must be generated, which is done by commercially available high voltage power amplifiers (Kepco, Typ BOP 1000M). But they have a rather limited bandwidth ($\sim 10 \text{ kHz}$). Therefore a pattern must be used which avoids the fast jump to the next line, as is the case in all television systems. Figure 2 shows the time dependence of the deflection voltages in x and y direction and the resulting pattern.

This pattern is generated similar to Ref. 4 in digital form by two up/down scalers whose registers give the values of the x and y coordinates. They are driven by a clock pulse generator which can be gated with the dead time of the secondary radiation analysis system to ensure equal measuring times for all points of the pattern. By a variable frequency dividing stage the time per point can be selected in a wide range between $10 \mu\text{sec}$ and 10 msec in steps of $10 \mu\text{sec}$.

Also the number of points in x and y direction can be selected to 1 or between 4 and 256 in binary steps, thus enabling line scans as well as area scans with a variable number of analysis points. For area scans the position of a toggle switch determines whether the pattern consists of lines or columns.

The x and y scaler registers are fed to an output buffer register that acts as address register for a multi-channel analyser. Moreover, the digital scaler information is converted to analog voltages by means of DACs to drive the high voltage power amplifiers of the deflection electrodes. Second parallel analog outputs may be used for the x and y deflection of a monitoring storage oscilloscope which is brightened^{4,5)} whenever the analysis system registers a specific secondary radiation.

The circuit of the pattern generator is assembled on seven boards as shown schematically in Figure 3. Detailed plans of the circuit boards are shown in Figures 4 to 7. Integrated circuits of the TTL-series (Texas Instruments, SN74LS) have been used exclusively. As all switches are coupled to the circuits via multipliers, their control can be taken over by a remote computer which must be furnished with a CAMAC system.

The output of the DAC converters (Burr-Brown DAC 80 CBI-V) are converted to low impedance with operational amplifiers (National Semiconductor, LH740) in a circuit shown in Figure 8. The potentiometer settings of analog gain and analog zero determine the length and origin of the sweep regardless of the digital setting of the number of analysis points.

All circuit boards are housed in a triple-width NIM module as shown in Figure 9.

4. APPLICATION EXAMPLES

To test the beam deflection system together with the pattern generator, different measurements have been performed. In the first test, the numbering in the corner of an integrated circuit has been scanned. The dimensions of this "number plate", shown in Figure 10a, are 1 x 0.4 mm. The characters with a line width of $\sim 40 \mu\text{m}$ are blank substrate of glass, while the rest of the plate is covered with a gold layer of $\sim 5 \mu\text{m}$ thickness. An areal scan of 32 x 32 points (point distance $\sim 9 \mu\text{m}$) covered the characters "27". The picture 10b is taken from the rear side after the irradiation and clearly shows the radiation damage of the beam, which has a penetration depth of $\sim 30 \mu\text{m}$, thus also penetrating the gold layer.

A single channel analyzer with the window covering the X-ray energy of the gold L-lines was used to gate a multi-channel analyzer connected to the address outputs of the pattern generator. In Figure 10c, the channel contents are plotted⁶⁾ perspectivevely representing the intensity distribution of gold. The grooves in the intensity reproduce the form of the two characters "27".

In a second test, the concentration profiles of different alloy compounds (Mo, V, Mn) have been determined across the boundary between a steel and a steel-alloy compound. By thermal treatment the migration of the alloy components into the steel region takes place. For such a problem, the line scan mode of the pattern generator is well adapted.

In the perspective plot⁶⁾ of Figure 11, viewed from two different sides, the one dimension represents the position across the boundary (channel width $\approx 3.3 \mu\text{m}$), while the other dimension gives the energy of the X rays detected with the analyzing system. The intensities, which are a measure of the concentrations, are plotted in logarithmic scale. The position of the boundary is marked, also the X-ray energies of the interesting alloy components. The decreasing concentration of molybdenum and vanadium with increasing distance from the alloy region is impressive. The bumps in the alloy region are caused by porosity and inhomogeneous grains in the alloy material.

ACKNOWLEDGEMENT

I thank Mr G. Pätzold for the careful realisation of the pattern generator. To Mr Kleykamp I am indebted for leaving the steel-alloy sample. Many thanks go to the van de Graaff operational staff for their permanent efforts to produce a high quality proton beam.

LITERATURE

1. D. Heck, Report KfK 2379 (1976) p. 108.
2. D. Heck, Report KfK 2504 (1977) p. 109.
3. D. Heck, Report KfK 2686 (1978) p. 115.
4. G. Bonani et al, Nucl. Instr. Meth. (1979), in print.
5. J.A. Cookson, A.T.G. Ferguson, F.D. Pilling, J. Radioanal. Chem. 12 (1972) 39.
6. O. Abeln, Program D3PLOT (1969), unpublished.

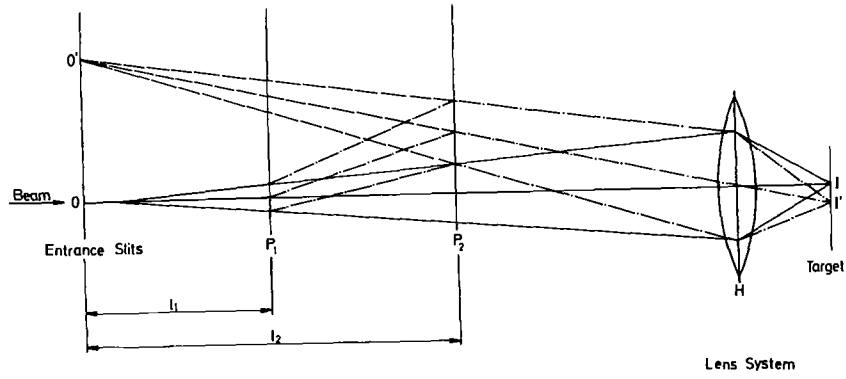


Figure 1. Scheme of the vertical deflection system.

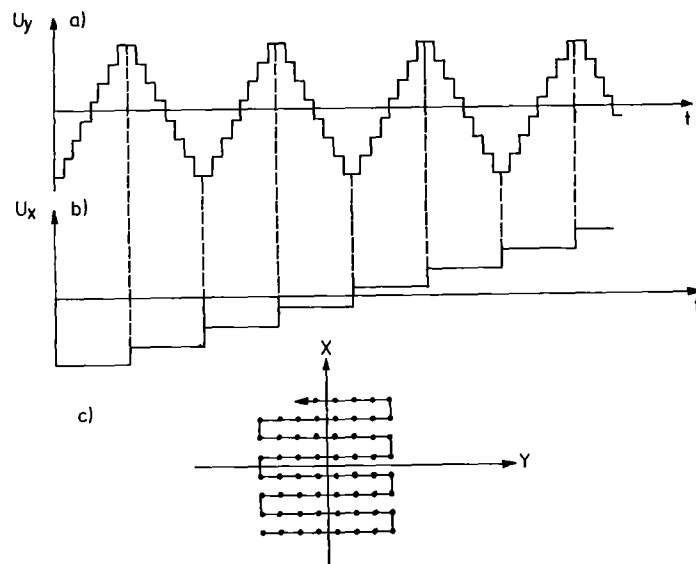


Figure 2. Time dependence of the deflection voltages and resulting scanning pattern.

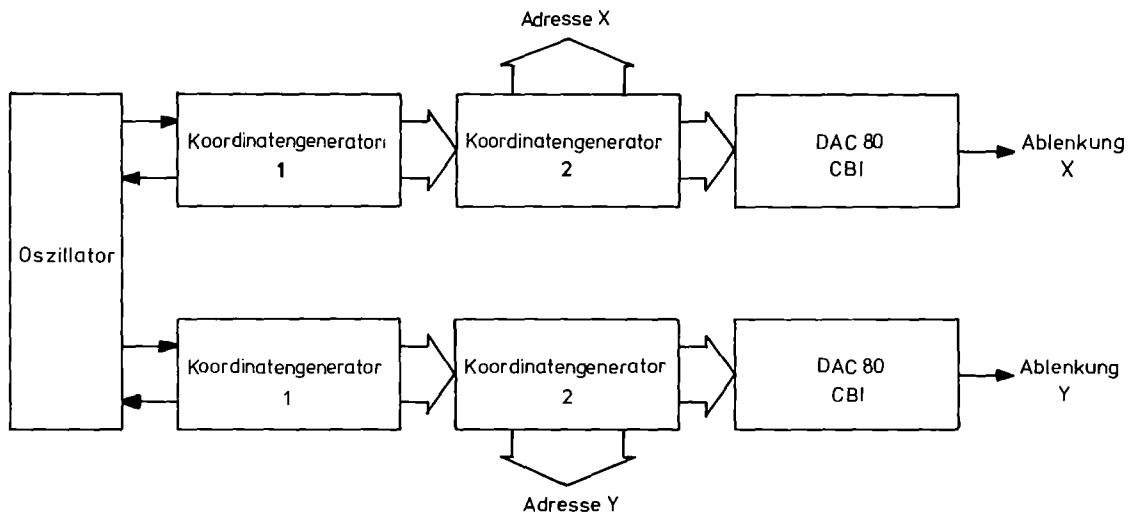


Figure 3. Block diagram of the pattern generator.

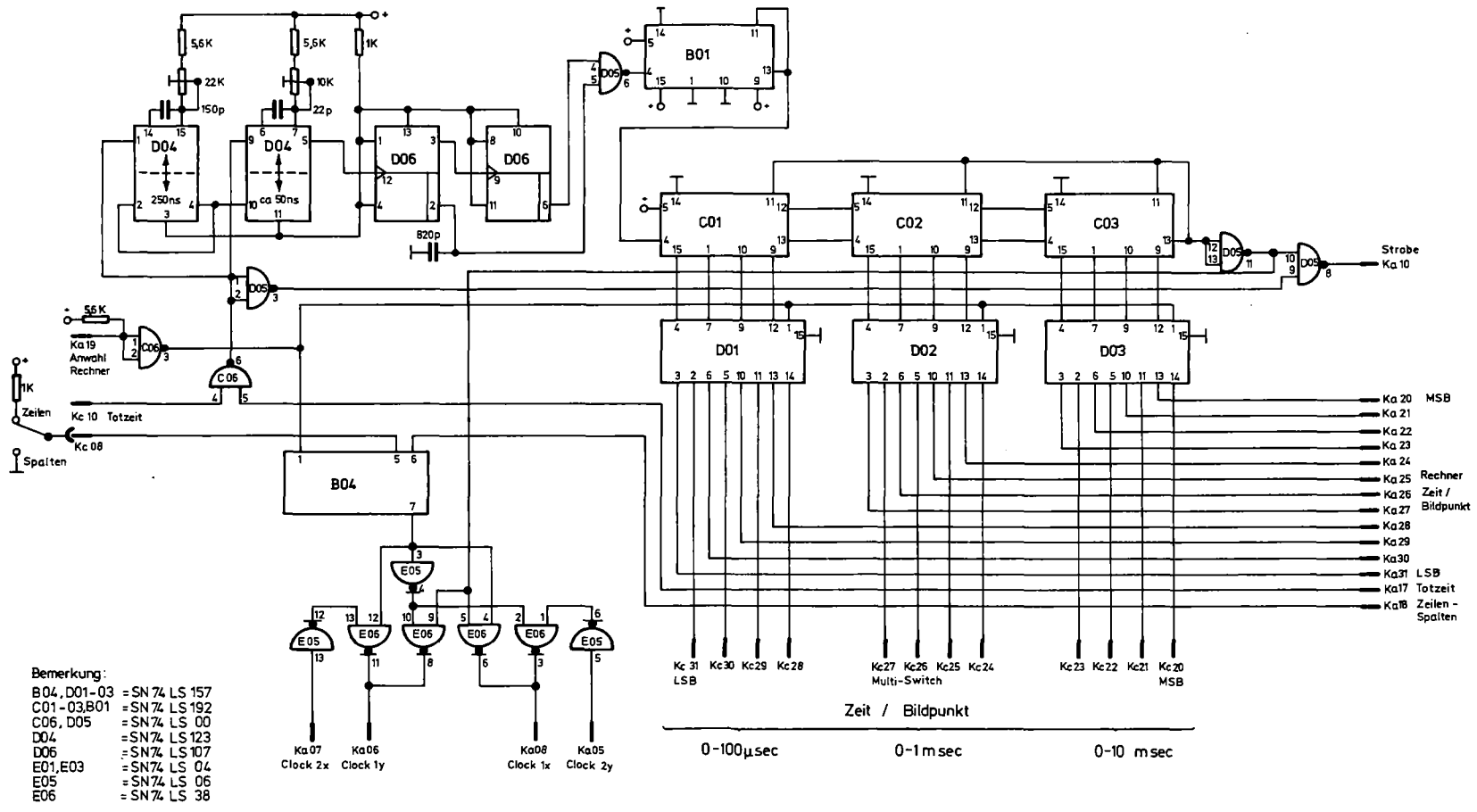


Figure 4. Oscillator and time per point circuit.

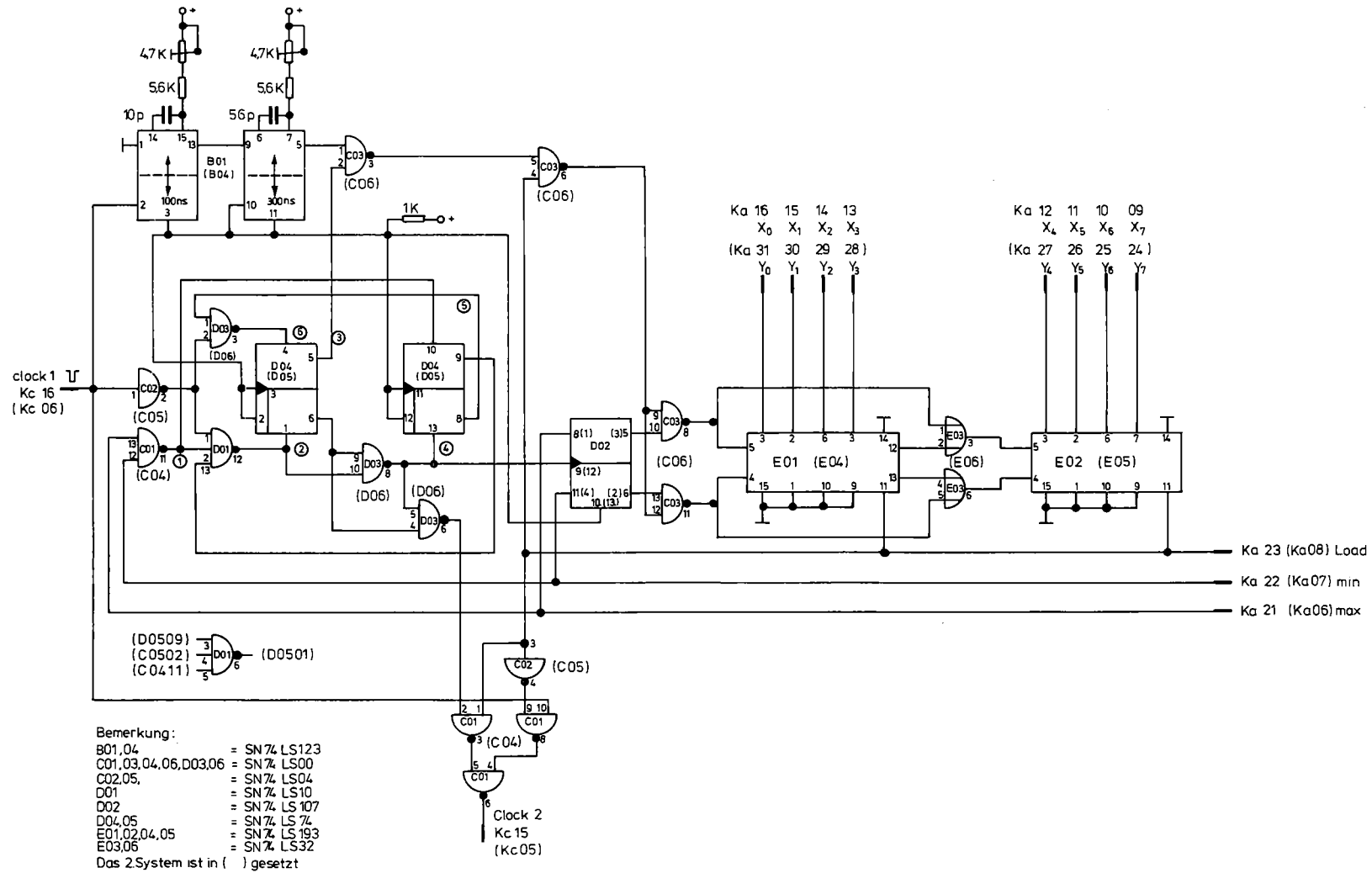


Figure 5. Up/down scaler and inversion circuit.

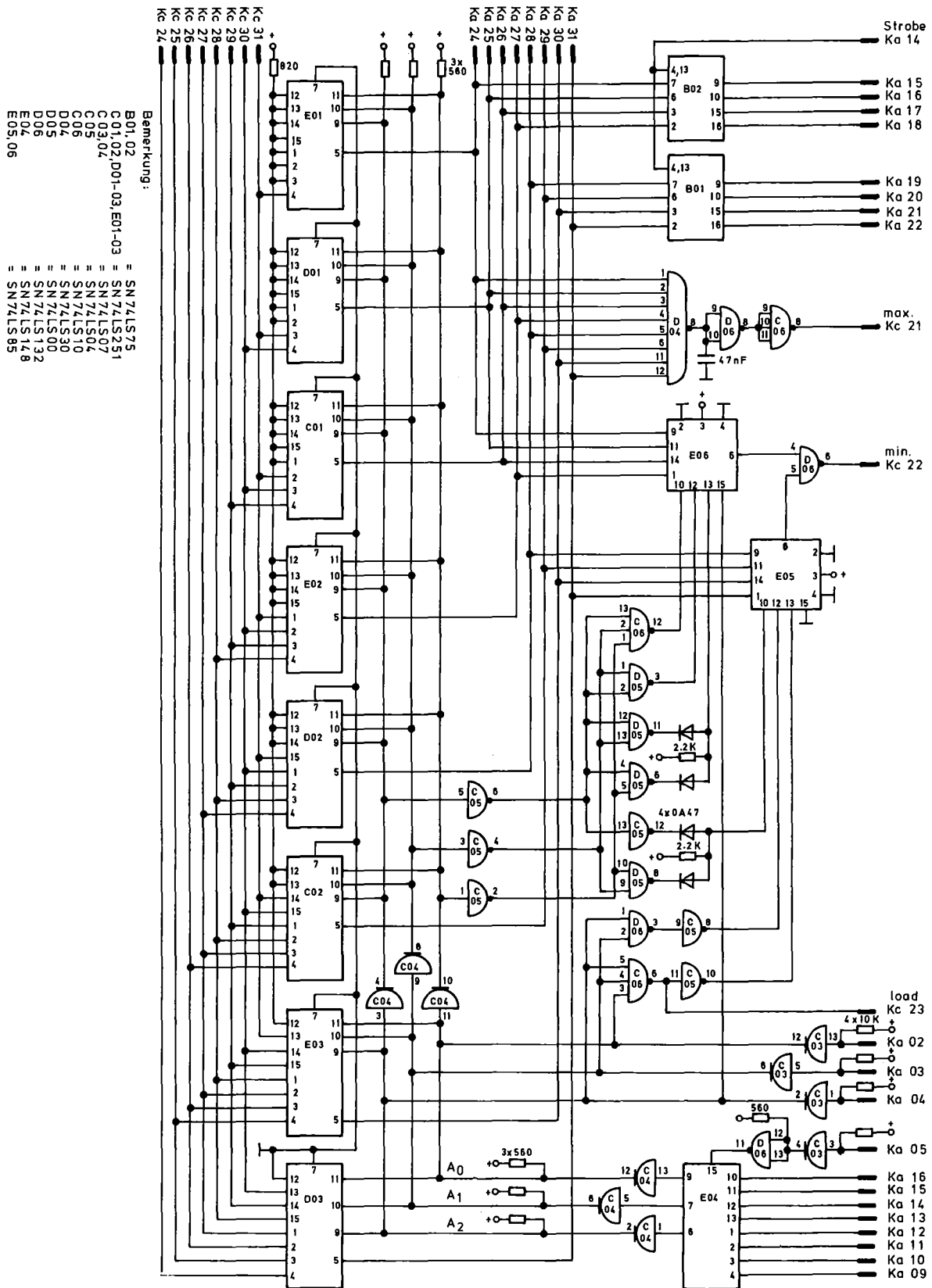


Figure 6. Bit shifter, address register and maximum/minimum generator circuit.

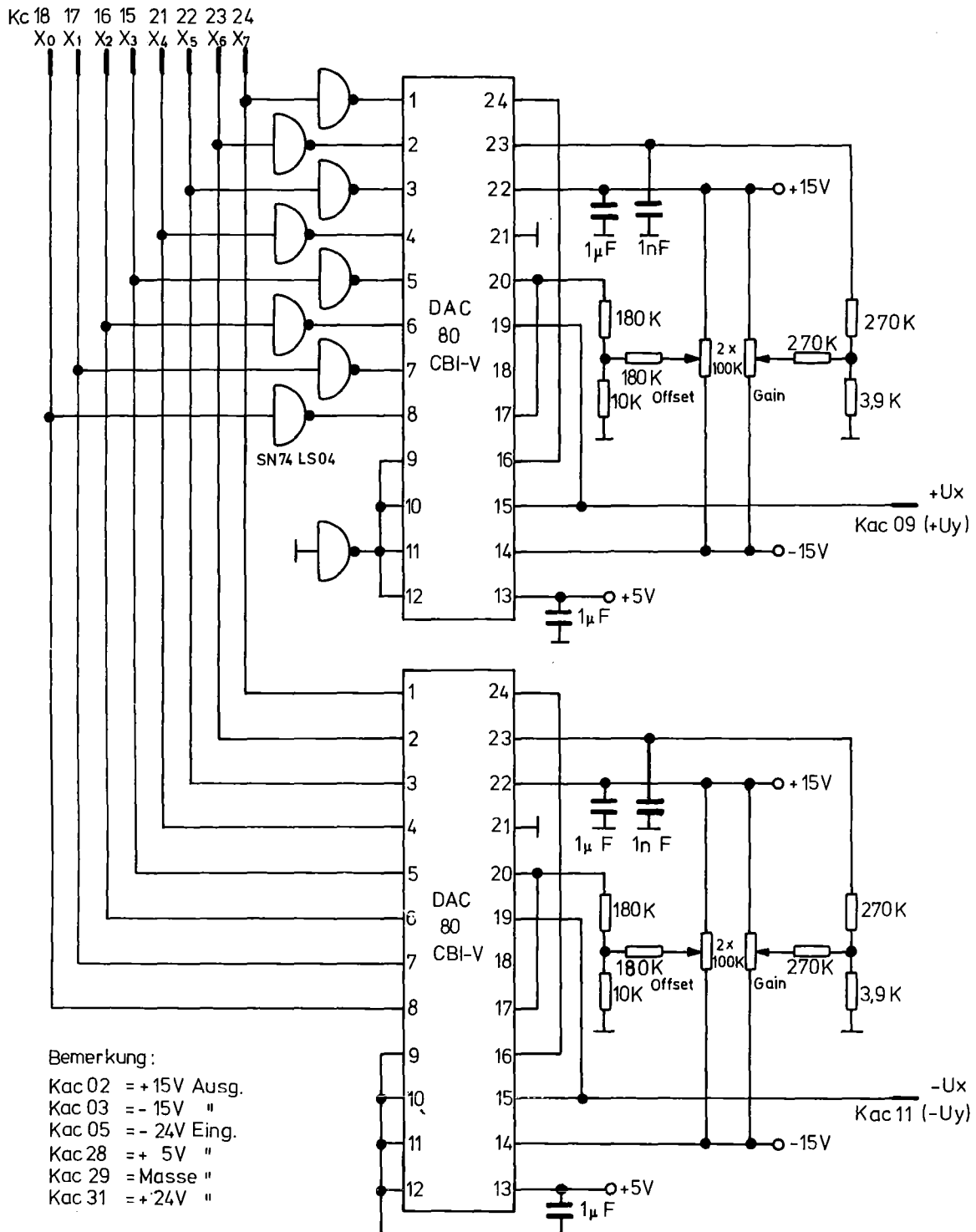


Figure 7. Digital analog converter circuit.

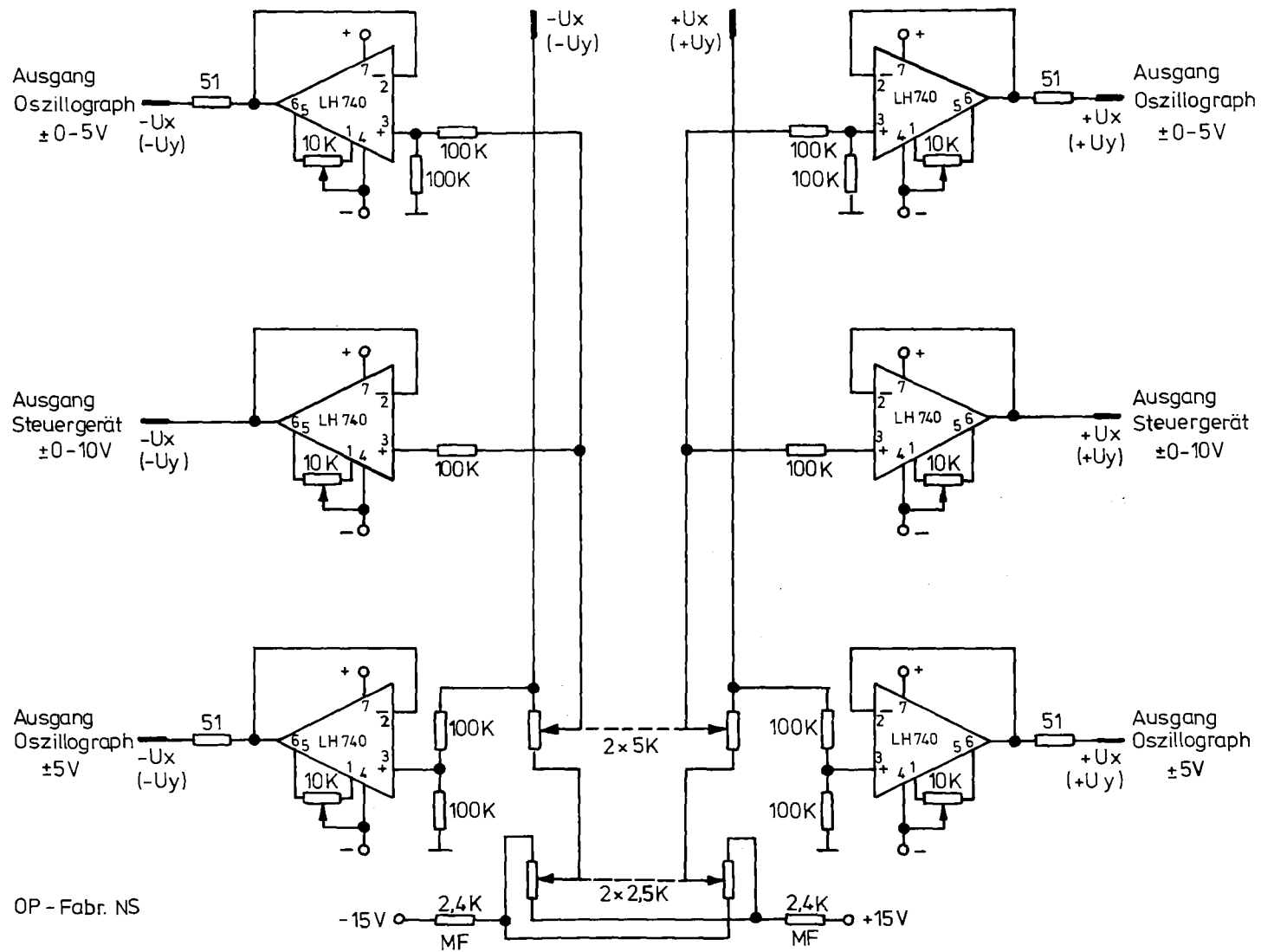


Figure 8. Output amplifier circuit.

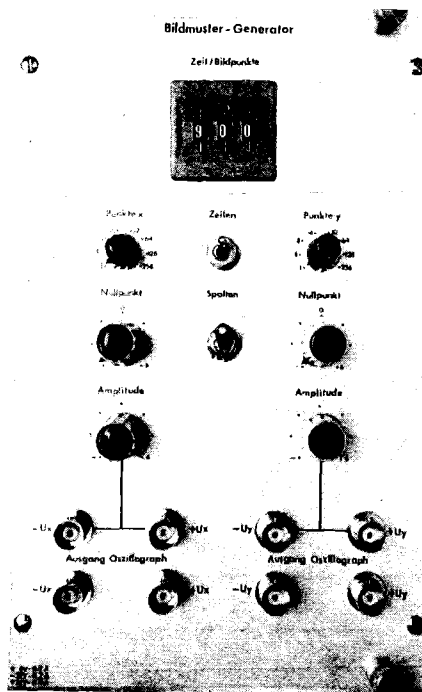


Figure 9. The pattern generator.

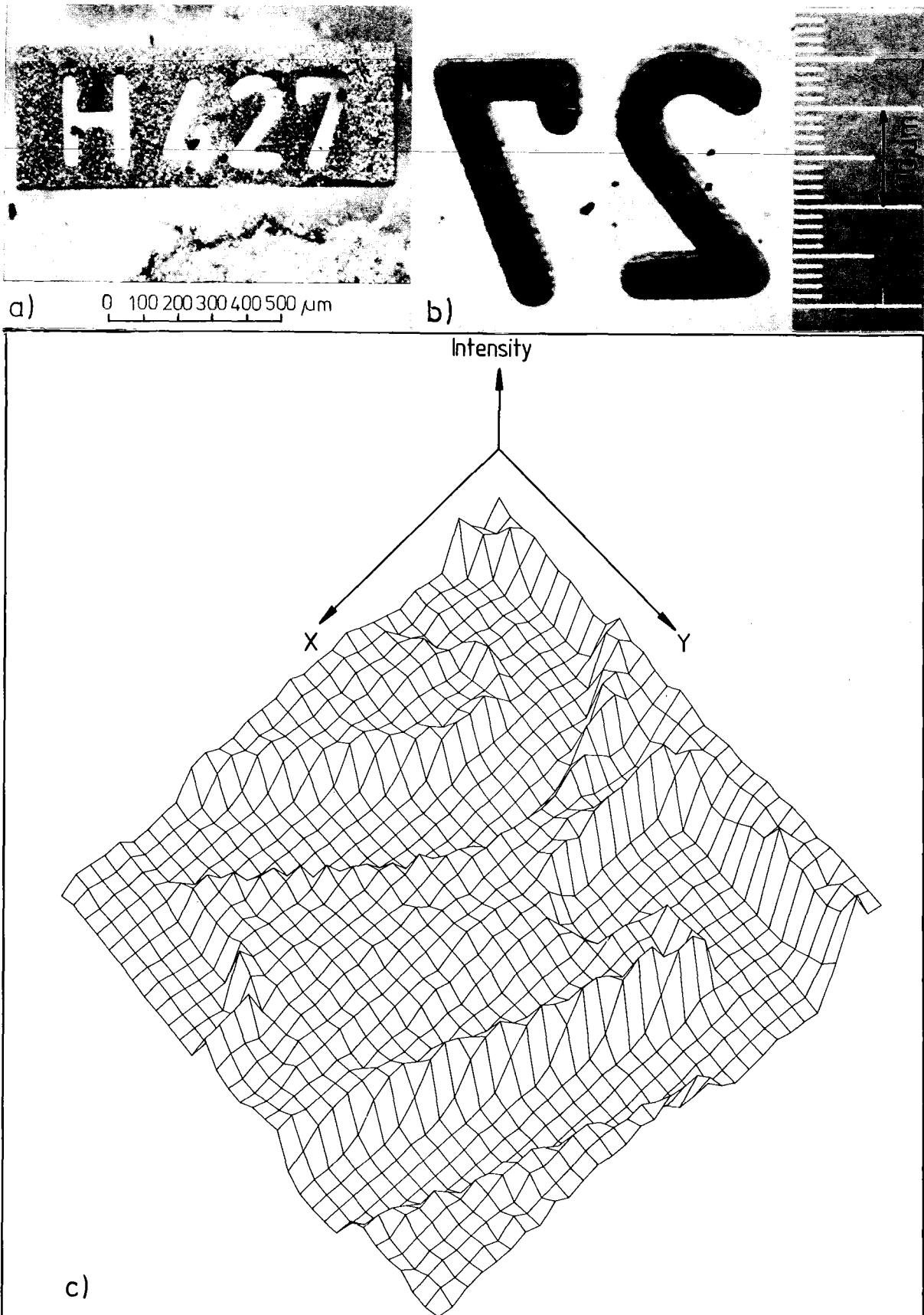


Figure 10. Number of an integrated circuit. a) Microphoto of the gold layer. b) Detail of "27" from the rear side with visible radiation damages. c) Two-dimensional channel array plot. The channel intensity gives information on the thickness of the gold layer.

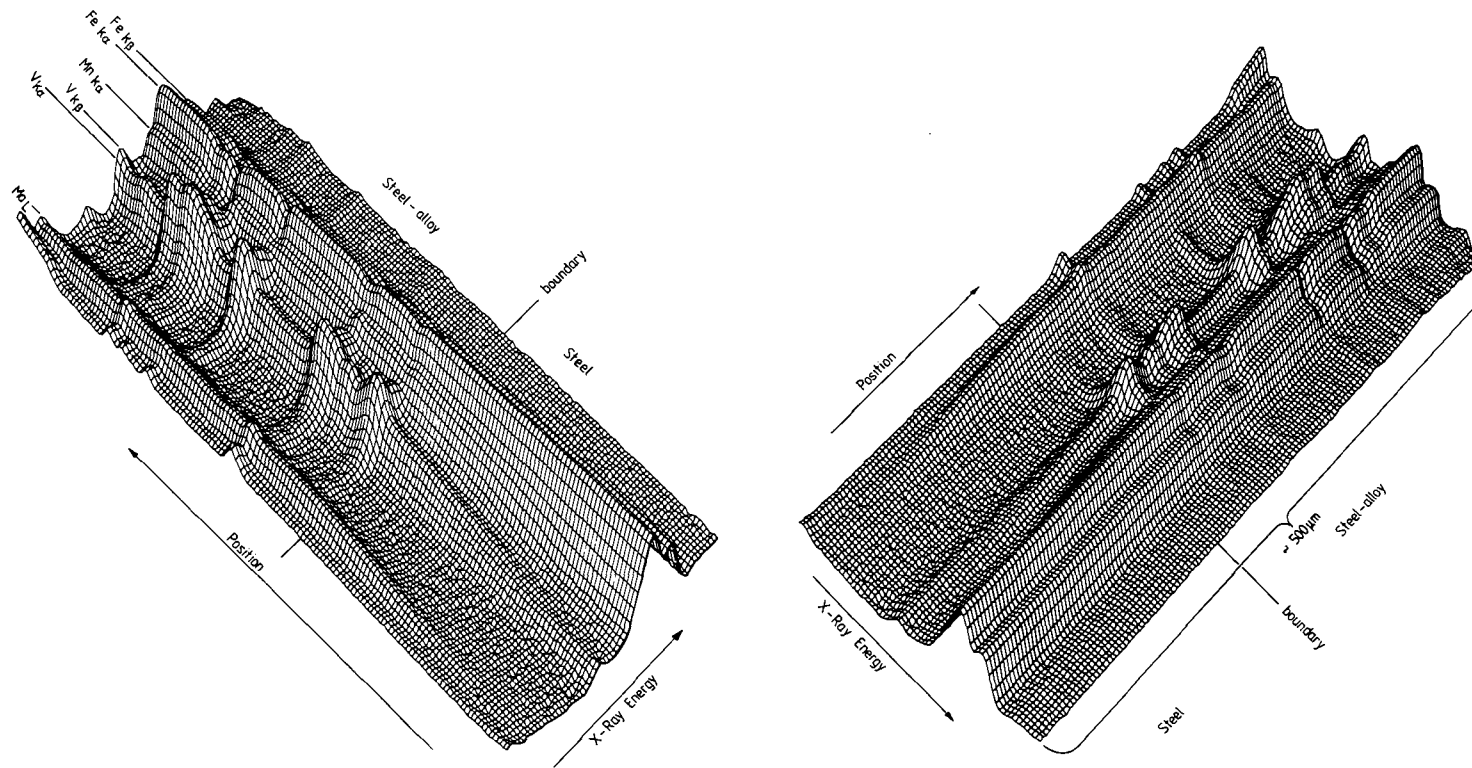


Figure 11. Perspective log-plot of the X-ray intensities across a steel/steel-alloy boundary.